Available online at www.sciencedirect.com

ScienceDirect

Procedia CIRP 26 (2015) 455 – 460

www.elsevier.com/locate/procedia

12th Global Conference on Sustainable Manufacturing

The use of Spark Plasma Sintering to fabricate a two-phase material from blended aluminium alloy scrap and gas atomized powder

Dimos Paraskevas[a,*], Kim Vanmeensel[b], Jef Vleugels[b], Wim Dewulf[a], Joost R. Duflou[a]

[a]*KU Leuven, Department of Mechanical Engineering, Celestijnenlaan 300A, B-3001, Heverlee, Belgium*
[b]*KU Leuven, Department of Materials Engineering, Kasteelpark Arenberg 44, B-3001, Heverlee, Belgium*

* Dimos Paraskevas. Tel.: +32-(0)16-372801; fax: +32/(0)16-322986. *E-mail address:* dimos.paraskevas@kuleuven.be

Abstract

Recently innovative solid state / 'meltless' recycling techniques have been developed and proposed for the consolidation of aluminium alloy scrap, aiming both at energy and material savings by eliminating the melting step. In this context, a powder metallurgy route is examined as a solid state recycling technique for the fabrication of a two-phase material via Spark Plasma Sintering. By mixing aluminium atomized powder and machining chips of the same alloy, a two-phase material was produced, where the powder phase acts as a binder/matrix for the Al scrap. Hardness, density, compression testing along with microstructural and computed tomography analysis of the densified Al 6061 alloy are presented.

Peer-review under responsibility of Assembly Technology and Factory Management/Technische Universität Berlin.

Keywords: Spark plasma sintering, aluminium alloys, recycling, powder metallurgy, machining chips.

1. Introduction

1.1. Challenges in aluminium recycling

A trend towards energy and resource efficient manufacturing could be observed in recent years driven by public concerns for environmental protection and resource conservation, but also as result of the prospective stricter policies on climate change avoidance [1]. In order to meet the global greenhouse-gas (GHG) targets, stabilizing the global average temperature at 2^0C above the pre-industrial level by 2050 and a reduction of GHG emission by 50-85% below year 2000 levels are required [2]. For the aluminium sector, a 50% total emissions reduction is translated into 85% decline to the emission-intensity, since global aluminium demand is expected to at least triple by 2050 [3]. This challenge can only be addressed by aiming at both energy and material/resource efficiency improvements [1,4].

Secondary aluminium from scrap requires much less energy than primary production. The theoretical energy to remelt and cast aluminium scrap is 1.14 MJ/kg [5]. However, despite considerable improvements in energy efficiency of the melting furnaces, the overall energy consumption of secondary aluminium production still can be as high as 7.7 MJ/kg [5] or 20 MJ/kg [6] depending on the type of aluminium scrap, the furnace technology and the production energy mix used.

Globally, 41% of liquid Al becomes process scrap, and in consequence does not directly become part of a functional product [4]. A scrap mass flow balance model presented by Boin and Bertam [7] for the EU in the reference year 2002 shows that 'turning scrap' (e.g. turnings, chips and cuttings) represents a relatively big flow of approximately 18% of the total industrial aluminium scrap mass. The recycling of this scrap category is considered to be problematic, mainly due to its high metal losses during remelting. Light-gauge scrap, having an extremely high surface area to volume ratio, tends to float on the surface of the melt. This causes significant oxidation losses of around 16% [8] or even up to 25% [9] that cannot be recovered since the metal property is lost. By avoiding the remelting, significant amounts of both energy and metal can be saved. Moreover, during the final recycling step of remelting, dilution losses (dilution with of scrap mixture with primary aluminium to reduce the concentration

Peer-review under responsibility of Assembly Technology and Factory Management/Technische Universität Berlin.
doi:10.1016/j.procir.2014.07.074

of impurities/residuals) as well as quality losses/down-cycling (loss of original functionality, reducing purity) occur that can limit the scrap usage [10]. A decision support tool for environmentally conscious metal management and improved scrap sorting has been developed, aiming in the minimization of those losses during recycling of Al [10].

1.2. 'Meltless' recycling techniques

Recently, various solid state recycling techniques have been developed, targeting aluminium scrap consolidation by plastic deformation [11-15]. This plastic deformation should be large enough to break-up the surface oxide layer of the chips in order to join clean and non-oxidized metal surfaces and allow the formation of adhesive metal bonds. Tekkaya et al. [11] and Güley et al. [12] hot extruded a cold pre-compacted Al alloy chips billet directly into profiles. The authors reported potential energy savings of nearly 90% compared to the conventional recycling route. Haase et al. [13] improved the solid state chips welding as well as the mechanical properties of the extrudates by introducing additional plastic strain into the material using an Equal Channel Angular Pressing (ECAP) die set during hot extrusion. Comparable tensile strengths and density as for reference base materials can be achieved following this approach. Widerøe et al. [14] developed a direct screw extrusion method of shredded scrap, introducing rotational movement to the scrap compacting and extruding in a single step. A different approach was presented by Sherafat et al. [15], who recycled Al 7075 alloy chips with the use of commercial air atomized, pure Al powder to fabricate a two-phase Al7075/Al material. The mixture of chips and powder was cold compacted and hot extruded in various mass fraction ratios.

Paraskevas et al. [16] used Spark Plasma Sintering (SPS), an advanced pressure assisted sintering method, as a novel solid-state recycling technique for the case of aluminium alloy scrap in form of chips. The technical feasibility of this approach was proven as well as the microstructure and the mechanical properties of the recycled material were investigated. The present study investigates the feasibility to recycle Al alloy chips with the aid of aluminium powder of the same alloy, at temperatures below the solidus, via SPS. In this approach, chips can partially substitute a mass fraction of the atomised powder in the sintered products. Fully-dense near-net-shape products can be directly produced via SPS, targeting both energy and material efficiency improvements.

1.1. Spark Plasma Sintering description

SPS is a pressure assisted, pulsed electric current Joule heated sintering method [16,17] recently pioneered in the field of powder metallurgy. SPS is also known as Field Assisted Sintering Technique (FAST) or Pulsed Electric Current Sintering (PECS), plasma pressure compaction, pulse electric discharge process, plasma activated sintering, electric field sintering, plasma pressure consolidation, pulse current pressure sintering and pulsed current hot pressing. SPS recently attracted considerable attention as a rapid sintering method capable of producing highly dense and homogeneous nanostructured sintered compacts and various advanced new materials in shorter sintering times than can be realised by conventional processing methods. The power consumption during SPS consolidation is about one-third to one-fifth of that of traditional techniques, including pressure-less sintering, Hot Pressing (HP) and hot isostatic pressing.

The applied pulsed electric current is combined with a uniaxial mechanical pressure to achieve very fast powder sintering. The pulsed current in the powder compact results in a very high thermal efficiency because of the direct volumetric heating of the sintering mold and especially the stacked powder material. In contrast to conventional HP, SPS is designed to have a very special power supply system as well as a special tool design that enables electrical current flowing directly through the compact and/or the die, depending on the electrical conductivity of the components. This allows very high heating and cooling rates with relatively low energy consumption [18].

Besides the benefit of direct volumetric Joule heating, the use of high current DC pulses may assist the consolidation process of difficult to sinter metal powders [17]. Aluminium/aluminium alloy powders are difficult to sinter due to the always present and stable surface oxide layer that inhibits bonding. SPS however has been successfully applied for aluminium powder consolidation, achieving full densification [19-20]. Despite some physical similarities with hot pressing (HP), SPS has demonstrated a potential to provide distinct technological and economic benefits over HP due to shorter processing times, reduced temperature and pressure requirements to achieve full density, and extremely high heating rates.

2. Materials and experimental procedure

2.1. Starting materials

Chips generated by dry machining of an Al 6061 alloy ingot in –0 temper (annealed), and gas atomized spherical powder (D_{10}=9.2, D_{50}=29.9 and D90=72.0 μm) of the same alloy were used as starting materials. A shaking device was used for mixing the chips/powder in a 50:50 ratio. The chemical composition of the Al 6061chips and 6061 gas atomized powder is comparable and presented in Table 1. Figure 2a-b presents the starting materials used.

Table 1: Chemical composition (wt %) of chips and powder

Element	Chips	Powder
Al	97.86	97.94
Fe	0.142	0.121
Si	0.695	0.692
Cu	0.278	0.249
Mg	0.989	0.979

2.2. Sintering cycle and tool set-up

The blended chips and atomized powder were cold pre-compacted in order to efficiently fill the SPS die. The SPS equipment (HPD 25/1, FCT Systeme, Frankenblick, Germany) consists of a 250 kN hydraulic press, a power supply system, a vacuum/gas chamber and a fully automated thermal and hydraulic process controller. Steel dies and punches (Uddeholm grade QRO 90), and a 0.35 mm thick

graphite paper (Carbone Lorraine grade N998) at the punch/die and die/aluminium interfaces were used. Graphite paper was also used between the punches and the metal to facilitate resistance heating and to avoid sticking of the compact to the punch and die. The use of graphite paper between the die and the powder compact and punches forces the current through the compact, hence improving the energy efficiency [18]. The process temperature was recorded and controlled by a flexible thermocouple (TC), positioned through a borehole at the bottom centre of the upper cylindrical punch, close to the sample. A molybdenum-titanium-zirconium (TZM) alloy was used for the protection plates of the punches. A photograph of the used SPS tool set-up is shown in Figure 1.

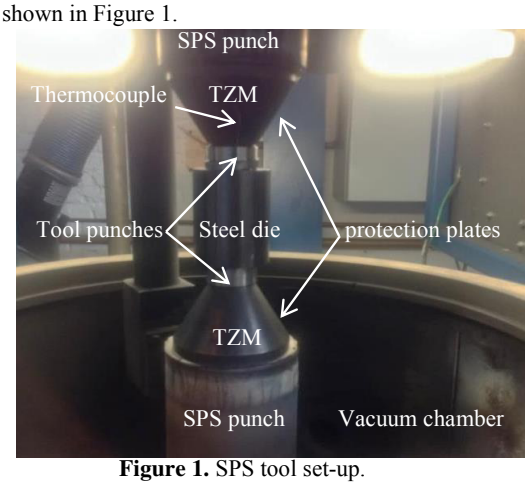

Figure 1. SPS tool set-up.

The sintering cycle consists of the creation of vacuum in the surrounding vessel, applying a pulsed current until 490^{0}C, application of a mechanical load, a dwell time under maximum mechanical load and a cooling step with subsequent release of the mechanical load. The sintering cycle is presented in Table 2. The 6XXX alloy range can age-harden and an artificial/accelerated aging treatment is usually implemented after hot processing (e.g. after hot extrusion). Therefore, an artificial aging step was performed in an air furnace at 175^{0}C for 4.5 hours based on the common industrial practice for this alloy. After the heat treatment step the SPS sample can be considered in -T5 temper state (cooled after high-temperature processing and artificially aged).

Table 2: The different segments of the sintering cycle

Different segments of the process					
Vacuum creation	Pulsed current heating 100^{o}C/min	Pulsed current heating 10^{o}C/min	Pressure application up to 200MPA	Dwell 490^{0}C/ 200MPA	Cooling

2.1. Hardness and density measurements

The Vickers hardness ($HV_{0.3kg}$) was measured on polished surfaces and cross-sections of the densified alloys. The reported values are the average and standard deviation of 5 indentations. The Vickers micro-hardness was determined using a hardness tester (model 3220, Zwick, Ulm, Germany) with 0.3 kg load and 10 s holding time. The density was measured by the Archimedes' method (immersion method).

2.2. Microstructural investigations

After typical metallographic preparation (grinding and polishing), the microstructure and the chemical analysis of the top and cross-section surfaces of the sample were performed by Scanning Electron Microscopy (SEM, XL-30FEG and FEI Nova Nanosem, FEI, The Netherlands) with a backscattered electron detector. Moreover, qualitative and quantitative Energy-Dispersive X-ray Spectroscopy (EDS) elemental analysis have been performed in order to identify the intermetallic phases.

2.3. X-ray industrial computed tomography

Computed Tomography (CT) is a non-destructive inspection technique based on differences in absorption/attenuation of X-rays through the material. The internal structure and a tomo-density analysis of a scrap/powder compacted sample were investigated using an industrial computed tomography (CT) installation (Nikon, XT H225). Residual micro-porosity, cracks, material homogeneity and impurities can be detected through non-destructive inspection by CT analysis. The sample was mounted on polyurethane foams and positioned in the CT device. The scans were configured at 140 kV and 145 μA. The obtained data were analyzed by means of the VGStudio MAX 2.2.1. software.

2.4. Compression testing

The mechanical behavior of the material was assessed by compression testing using an Instron model 4467 device. For this reason 5 specimens (Ø= 6 mm and 9 mm height) were cut by wire electrical discharge machining (EDM) out of the sintered compact (see Figure 2c).

Prior to EDM, the sintered compacts were ground plan parallel. Compression tests were performed using a constant displacement control (0.2 mm /min) at room temperature. The corresponding ASTM standard was followed for the compression tests [21]

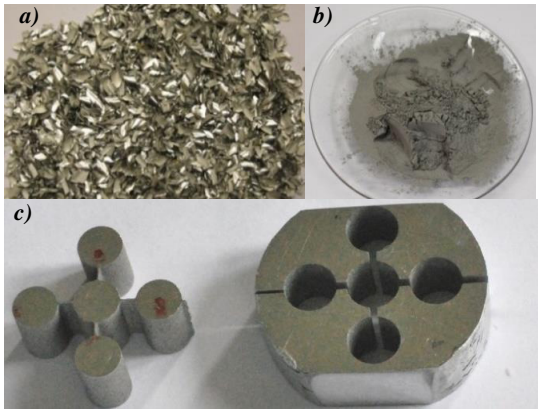

Figure 2: a) AA6061 machining chips, b) AA6061 atomized powder, c) SPS disc and compression test specimens.

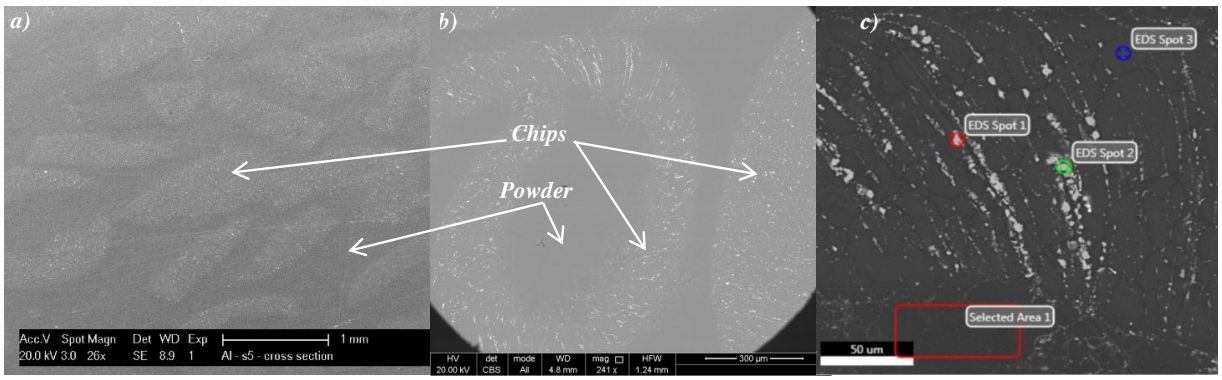

Figure 3: SEM micrographs of a) cross-sectioned surface, b) top surface, and c) higher magnification revealing the intermetallic compounds in the "chips".

3. Results

3.1. Microstructural investigations

Figure 3 presents the microstructure of the top surface (Fig.3a) and the cross-section (Fig. 3b) of the SPS disc. Figure 3c shows the intermetallic phase particles in the "chips" (bright spots due to their higher density). Copper intermetallic compounds were measured in the EDS spots 1 and 2 (53.4 %wt and 45.19 %wt respectively). The leftovers of the chips are highlighted by the brighter intermetallic compounds (Fig. 3c). The intermetallics clearly align the chip form and boundaries. Good bonding has been achieved between the chips and powder resulting in a fully dense material. Only one area with some small pores of a few μm was observed in the cross-section (see Figure 4). Apart from this region, no other micro-porosity/voids have been observed in the disc by means of scanning electron microscopy.

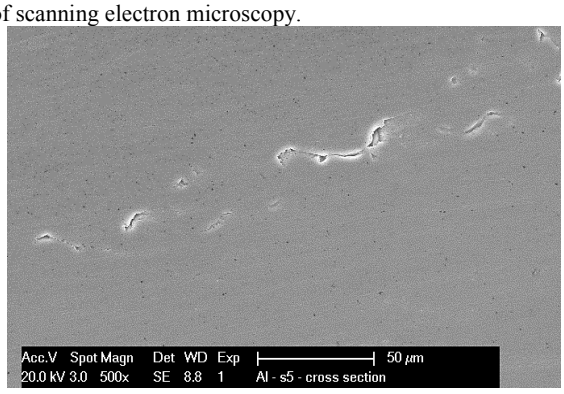

Figure 4: SEM micrographs of micropores observed in a cross-section sample.

3.2. Density and hardness results

The density of the SPS discs measured by the Archimedes method was 2.70 g/cm^3, identical to the theoretical density of aluminium alloys. The material can be considered as fully densified. However, since Al_2O_3 has a higher density than Al (3.98 g/cm^3), a slightly lower value than 100% TD is expected due to the oxide content of the chips.

The micro-hardness after artificial aging was 713.2±28.4 MPa on the top surface and 661.2±35.3 MPa on a cross-section. The hardness of the reference 6061 alloy ingot used to generate the chips was 709.3±20.6 HV. The small value of the standard deviation (σ) on the hardness values indicates a homogeneous material.

3.3. X-Ray Industrial Computed Tomography (CT) analysis

The CT images in Figure 5 reveal the presence of two phases due to the different X-rays absorption capacity by the powder and the chips. The produced SPS sample was CT scanned for internal structure evaluation. The derived 3D model of the specimen was analysed slice per slice obtaining the full picture of the sample.

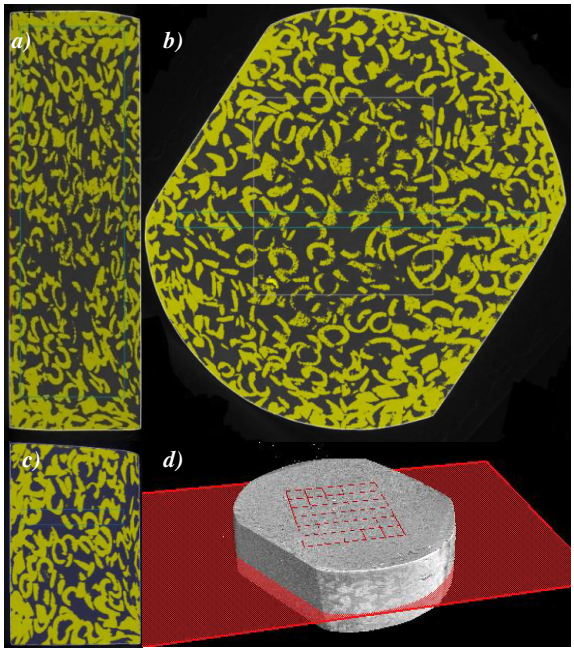

Figure 5: CT images presenting a three-view typical slice of the SPS sample. a) xz plane, b) xy plane, c) yz plane and d) an overview of the sample.

The whole set of cross-sectional frames was post processed. The bulk area was packaged into video clips in the three planes (xy, xz, yz). Figure 5 provides three view images and a sample overview in which no pores can be identified. An in-depth analysis revealed that the CT measurement has a voxel size of 21.7 μm in the X,Y and Z direction. For visual detection, a size of at least three voxels is required. Assuming a spherical porosity would imply a threshold radius of 32.6 μm.

The absorption of the chip and powder phase is slightly different resulting into two different peaks in the grey value (see figure 6). The chip phase having higher grey value is marked yellow and the powder phase grey (see figure 5). From a volume analysis, the chips volume fraction was measured around 47%, which is in good agreement with the 50/50 ratio that was initially loaded in the steel die. The CT findings confirm a sound solid state welding capacity of the SPS process since no porosity (>35 μm) was detected within the global sample structure. A relative homogeneous distribution of the chips can be observed.

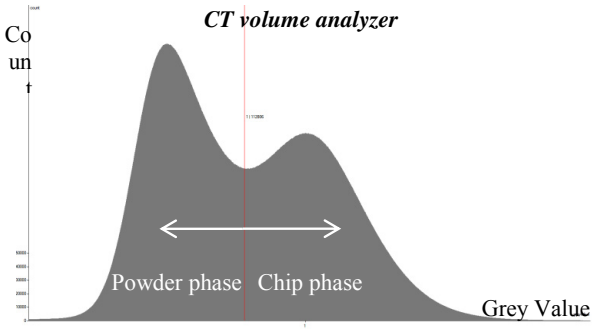

Figure 7: Grey value of the two phases in the CT volume analyzer.

3.4. Compression testing

The true stress-strain compression curves of the specimens taken from the periphery (P1-4) and the center of the SPS sample, as well as for the parent material used for the chip production (Al606-T0) as reference, are shown in Figure 7. None of the specimens failed during compression testing up to 45% true strain, implying a good ductility and sound welding of powder particles and chips. During compression in the plastic region, the compression specimens attained a 'barrel' shape. This phenomenon is known as 'barrelling' and occurs as the frictional force is not constant over the entire cross-section of the specimen and varies from a minimum at the center to a maximum at the edges.

For ductile metals, compressive strengths can be derived from the stress-strain curve at specified total strains [21]. The total elongation of the Al6061 T6 is between 12-17% [22]. Since necking during tensile loading will occur earlier and the SPS sample is in T5 temper, the compressive strength is reported at different strains between 7-12%. Table 3 summarizes the mechanical properties of the SPS sample based on the analysis of true stress-strain curves.

The average values of the 5 specimens along with their standard deviations are shown. The increased Yield strength of the SPS sample compared with the reference Al-6061 T0 is due to the artificial aging step where the SPS material gained properties. Generally, the mechanical properties of the SPS sample after the artificial aging step can be considered as comparable with the Al6061–T5 temper properties [22].

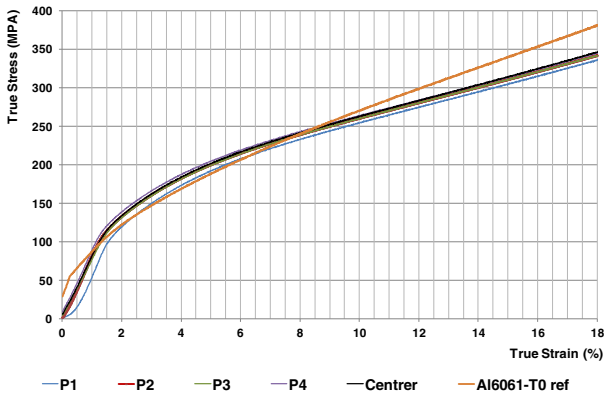

Figure 7: True stress-strain compression curves.

Table 3 presents also the strain hardening exponent (n) which is a material constant used in calculations for stress-strain behaviour in work hardening. In the formula $\sigma = K\varepsilon^{n}$, σ represents the stress on the material, ε is the strain, K is the strength coefficient. The value of n is between 0, that means that a material is a perfectly plastic solid, and 1 that represents a 100% elastic solid. The strain hardening exponent obtained as the linear slope of a ln(stress) versus ln(strain) curve in the plastic region.

Table 3: Mechanical properties.

	Values ± σ	Comment
Yield strength (0.2 proof stress)	120.6 ± 3.6 MPa	70 MPa the ref. Al6061-T0
Compressive Strength	228 ± 3.5 MPa	at 7% true strain
	237.8 ± 4 MPa	at 8% true strain
	248.8 ± 3.1 MPa	at 9% true strain
	259.4 ± 3.6 MPa	at 10% true strain
	269 ± 4.3 MPa	at 11% true strain
	280.6 ± 4.5 MPa	at 12% true strain
Strain hardening exponent (n)	0.4 ± 0.02	0.49 the reference Al6061-T0
Strength coefficient (K)	103.7 MPa	86 MPa the ref. Al6061-T0

1. Conclusions - Discussion

A chips and gas atomized powder mixture of the same aluminium alloy was consolidated well below the solidus temperature resulting into a fully dense two-phase material. Light gauge Al scrap category is connected with much higher metal losses during conventional recycling compared to the other scrap categories, making it ideal feedstock material for solid state recycling. Utilizing SPS, scrap consolidation was achieved with the aid of gas atomized powder at a temperature of only 490°C, without material losses. After the

sintering cycle the SPS material was artificially aged obtaining mechanical properties comparable with the –T5 tempered material.

Aluminium powder acts as a binder and matrix providing a better bonding for the chips and excluding residual porosity. Five compression test specimens were taken from the periphery and the center of the SPS densified disc. The samples had a homogeneous hardness and comparable behavior during compression with low variations in the stress-strain curves, despite a locally different powder/chip phase ratio as revealed by CT images. The authors believe that the use of chips and powder of the same alloy aids in the direction of obtaining homogenous properties within the material as it consists of two different phases. Moreover, the homogeneous mechanical properties of the two-phase material are a proof of the homogeneous temperature distribution within the material during sintering. Insulating the die from the compact and punches by graphite paper forced the current through the compact, hence improving the energy efficiency [18].

Summarizing, the use of SPS as a solid state welding technique for fine form Al scrap with Al powder is technically feasible, highly promising and worth further future exploration. SPS can fracture and disperse the surface oxides of the Al chips, desorb the entrapped gases and activate the metallic surfaces of powder particles and chips resulting in fully dense near-net or even final shape sintered products. Single alloy fine form scrap can effectively substitute a mass fraction of the much more expensive atomized aluminium alloy powder in sintered products, decreasing its production cost. Concerning the valorization potential of the observed process performance, single alloy fine form scrap can effectively substitute a mass fraction of the much more expensive atomized aluminium alloy powder in sintered products, decreasing its production cost.

Acknowledgements

The authors acknowledge support of the research fund of KU Leuven through project GOA/15/012-SUMMA. The authors also thank ALPOCO for providing the gas atomized powder.

References

[1] Gutowski, T., Allwood, J.M., Sahni, S. and Herrmann, C., 2013. A Global Assessment of Manufacturing: Economic Development, Energy Use, Carbon Emissions, and the Potential for Energy Efficiency and Materials Recycling. Annual Review of Environment and Resources, 38: 81-106.

[2] IPCC Climate Change 2007: Mitigation of Climate Change (eds Metz, B.,Davidson, O. R., Bosch, P. R., Dave, R. & Meyer, L. A.) (Cambridge Univ.Press, 2007).

[3] Liu, G., Bangs, C.E., Müller, D.B., 2013. Stock dynamics and emission pathways of the global aluminium cycle. Nature Climate Change, 3:338-342.

[4] Milford, R.L., Allwood, J.M., Cullen, J.M., 2011. Assessing the potential of yield improvements, through process scrap reduction, for energy and CO2 abatement in the steel and aluminium sectors, Resources, Conservation and Recycling, 55/12:1185-1195.

[5] European Aluminium Association, 2008. Environmental Profile Report for the European Aluminium Industry, Life Cycle Inventory data for aluminium production and transformation processes in Europe.

[6] Schwarz, H.G., 2004. Aluminum production and energy, Encyclopedia of Energy, pp. 812004.

[7] Boin, U.M.J., Bertram, M., 2005. Melting Standardized Aluminium Scrap: A Mass Balance Model for Europe, JOM: Journal of the Minerals, Metals and Materials Society, 57/8:26–33.

[8] Xiao, Y., Reuter, M.A., 2002. Recycling of distributed aluminium turning scrap, Minerals Engineering, 15/1(1):963-970.

[9] Geertruyden, Van W.H., Prescott, C.A., Misiolek, W.Z., Peterson. R., 2005. Light Met. Age Band, 63 (6):14–18.

[10] Paraskevas, D., Kellens, K., Dewulf, W., Duflou, J.R., 2014. Environmental modelling of aluminium recycling: a Life Cycle Assessment tool for sustainable metal management, Journal of Cleaner Production http://dx.doi.org/10.1016/j.jclepro.2014.09.102

[11] Tekkaya, A.E., Schikorra, M., Becker, D., Biermann, D., Hammer, N., Pantke, K., 2009. Hot profile extrusion of AA-6060 aluminum chips, Journal of Materials Processing Technology, 209:3343-3350.

[12] Güley, V., Ben Khalifa, N., Tekkaya, A.E., 2010. Direct Recycling of 1050 aluminium scrap material mixed with 6060 aluminium alloy chips by hot extrusion, Int. Journal Material Forming, 3/Suppl 1:853– 856.

[13] Haase, M., Ben Khalifa, N., Tekkaya, E.A., Misiolek, W.Z., 2012. Improving mechanical properties of chip-based aluminum extrudates by integrated extrusion and equal channel angular pressing (iECAP), Materials Science and Engineering: A, 539:194–204.

[14] Widerøe, F., Welo, T., Vestøl, H., 2010. A new testing machine to determine the behaviour of aluminium granulate under combined pressure and shear, Int. Journal of Material Forming, 3/suppl. 1:861-864.

[15] Sherafat, Z., Paydar, M.H., Ebrahimi, R., 2009. Fabrication of Al7075/Al, two phase material, by recycling Al7075 alloy chips using powder metallurgy route, Journal of Alloys and Compounds, 487:395-399.

[16] Paraskevas, D., Vanmeensel, K., Vleugels, J., Dewulf, W. Deng, Y., Duflou, J.R., 2014. Spark Plasma Sintering As a Solid-State Recycling Technique: The Case of Aluminum Alloy Scrap Consolidation, Materials, 7(8): 5664-5687.

[17] Mamedov, V., 2002. Spark plasma sintering as advanced PM sintering method, Powder Metallurgy, 45(4): 322-328.

[18] Vanmeensel, K., Laptev, A., Hennicke, J., Vleugels, J., Van der Biest, O., 2005. Modelling Of The Temperature Distribution During Field Assisted Sintering, Acta Materialia, 53: 4379–4388.

[19] Sastry, K.Y., Froyen, L., Vleugels, J., Van der Biest, O., Schattevoy, R., Hennicke, J., 2004. Mechanical milling and field assisted sintering consolidation of nanocrystalline Al-Si-Fe-X powder, Reviews on Advanced Materials Science, Vol. 8 pp 27-32.T.

[20] Le, G.M., Godfrey, A., Hansen, N., 2013. Structure and strength of aluminum with sub-micrometer/micrometer grain size prepared by spark plasma sintering, Materials & Design, 49: 360-367.

[21] ASTM standard E9-89a, 'Standard Test Methods of Compression Testing of Metallic Materials at Room Temperature', ASTM International, West Conshohocken, PA, 2008, www.astm.org.

[22] CES EduPack.

Available at: http://www.grantadesign.com/education/